

Exact analysis of bi-directional functionally graded beams with arbitrary boundary conditions via the symplectic approach

Li Zhao^{**1}, Jun Zhu^{*2} and Xiao D. Wen³

¹Department of Civil Engineering, Ningbo University of Technology, No. 89 Cui bai Road, Ningbo, P.R. China

²College of Mechanical Engineering, Zhejiang University of Technology, Hangzhou 310014, P.R. China

³College of Electrical and Information Engineering, Yunnan Minzu University,
No. 121 YIERYI Avenue, Kunming, P.R. China

(Received November 7, 2015, Revised February 24, 2016, Accepted March 15, 2016)

Abstract. Elasticity solutions for bi-directional functionally graded beams subjected to arbitrary lateral loads are conducted, with emphasis on the end effects. The material is considered macroscopically isotropic, with Young's modulus varying exponentially in both axial and thickness directions, while Poisson's ratio remaining constant. In order to obtain an exact analysis of stress and displacement fields, the symplectic analysis based on Hamiltonian state space approach is employed. The capability of the symplectic framework for exact analysis of bi-directional functionally graded beams has been validated by comparing numerical results with corresponding ones in open literature. Numerical results are provided to demonstrate the influences of the material gradations on localized stress distributions. Thus, the material properties of the bi-directional functionally graded beam can be tailored for the potential practical purpose by choosing suitable graded indices.

Keywords: bi-directional functionally graded materials; analytical elasticity solutions; symplectic approach; state space; eigenfunction

1. Introduction

Due to astonishing advances in science and technology, new structural materials have attracted attention of numerous researchers. Functionally graded materials (FGMs) are a new generation of special non-homogenous materials, which have striking advantages over traditional homogeneous materials. FGMs are generally made from a mixture of two or more materials, whose material properties are varied continuously and smoothly along certain direction(s), thus reducing cracking and delamination phenomenon often observed in conventional composite materials. Typically, FGMs made of ceramic and metal can survive in environments with high-temperature gradients because of better thermal resistance of the ceramic phase, while maintaining stronger mechanical performance of metal phase.

The concept of FGMs was first introduced and proposed by a group of Japanese scientists

*Corresponding author, Ph.D., E-mail: zhujun@zjut.edu.cn

**Corresponding author, Ph.D., E-mail: zhaolinbc@163.com

(Koizumi 1993) and the original application of FGMs is for thermal barrier system (Koizumi 1997). In recent years, FGMs have been widely used in many engineering applications such as aircrafts, space vehicles, marine, civil construction, nuclear power plants and even micro/nano-electro-mechanical system. Many studies have been performed extensively to analyze the static behavior (Sankar 2001, Sallai *et al.* 2009, Simsek 2009, Neves *et al.* 2011, Simsek 2013), bucking behavior (Huang and Li 2011, Shahba *et al.* 2011, Simsek and Reddy 2013) and dynamic behavior (Khalili *et al.* 2010, Simsek and Cansiz 2012) of functionally graded structures. It can be seen from the literature that considerable attention are focused on the functionally graded structures with properties graded in one direction, especially in thickness direction (Reddy 2000, Ferreira *et al.* 2006, Ding *et al.* 2007, Huang *et al.* 2009). Recently, Shahba *et al.* (Shahba *et al.* 2011, 2012, Shahba and Rajasekaran 2012) presented the stability and free vibration analyses of axially functionally graded beams. The static analyses of FGM beams with material properties varying along the axial direction have also been presented (Zhao *et al.* 2012a, b). Chu *et al.* (2015) proposed a theoretical approach to solve the plane elasticity problems of FGMs with the material properties dependent on the thickness-wise direction or the width-wise direction in form of an exponential function.

In advanced nowadays structures such as modern aerospace shuttles and craft, there are elements which subjected to thermal and mechanical loads varying in two or even three directions. In the practice occasions, the conventional FGMs are not qualified to resist severe variations of temperature in multi-directions. Therefore, FGMs with two-dimensional and three-dimensional dependent material properties have more effective material resistant (so-called Bi-directional FGMs and tri-directional FGMs). Recently, a few researchers have investigated the thermo-mechanical and dynamic behaviors of multi-directional FGMs using various mathematical models. Nemat-Alla (2003) investigated thermal stresses of bi-directional functionally graded aerospace shuttles and craft using finite element method. Hedia (2005) extended the finite element model to stress analysis of bi-directional FGM structures. Sutradhar and Paulino (2004) developed a simple boundary element method for the transient heat conduction in multi-dimensional FGMs. Kuo and Chen (2005) derived Green's functions for steady-state or transient-state heat conduction in anisotropic bi-directional FGMs. Qian and Batra (2005) using the meshless local Petrove Galerkin method to obtain numerical solutions for static, free, and forced vibrations of a bi-directional cantilever beam. Lü *et al.* (2008, 2009) obtain semi-analytical elasticity solutions for bi-directional FGM beams and plates adopting differential quadrature method. Sobhani Aragh *et al.* (2011) presented the semi-analytical solution for free vibration and vibrational displacements of bi-directional FGFR curved panel. Nie and Zhong (2010) investigated the dynamic behavior of multi-directional functionally graded annular plates. Shariyat and Alipour (2013) employed the differential transform method to vibration analysis of circular plates with two-directionally graded materials. Ebrahimi and Najafizadeh (2014) analyzed the free vibration of a two-dimensional functionally graded circular cylindrical shell. Simsek (2015) studied free and forced vibration of BDFG beam due to a moving load by using the energy approach. Lezgy-Nazargah (2015) investigated the coupled thermo-mechanical behavior of bi-directional FGM beams using a modified finite element model.

It is noted that in majority studies mentioned above, the bi-directional or tri-directional FGMs are modeled by employing numerical and semi-analytical theories. There are few of investigation available in the literature on structural response of bi-directional FGM structures by means of analytical method. The symplectic framework in the Hamiltonian system developed by Zhong (1995), Yao *et al.* (2009) has shown great superiority in revealing the structure of solutions and

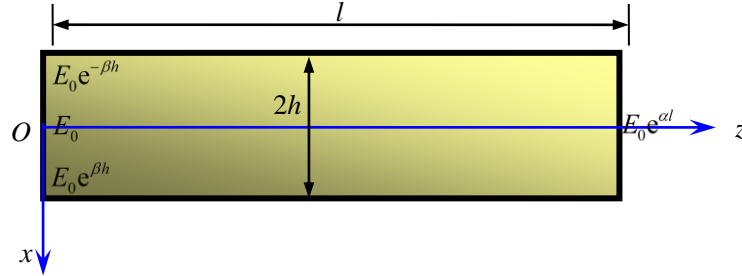


Fig. 1 The rectangular domain of bi-directional FGM problem

their physical essence as well as predicting the accurate local behavior. Zhao *et al.* (2012c) first proposed a symplectic formulation based on the state-space formalism for static analysis of bi-directional FGM beams with homogenous lateral conditions. This paper attempts to further extend the symplectic approach to the exact analysis of bi-directional FGM beams with various end conditions. On the basis of the particular solution which is derived from the eigen-function, analytical elasticity solutions of bi-directional FGM beams subjected to arbitrary distribution lateral loads are obtained in a systematically manner. Numerical results are presented to reveal effective and accurate of the present approach in predicting local stress distributions. The influences of the material gradient indices on the stress distributions are investigated.

2. Theory and formulation

We consider an isotropic elastic bi-directional functionally graded beam with length l and thickness $2h$. A Cartesian coordinate system is introduced such that the x -axis is aligned with the thickness axis and z -axis with the longitudinal direction as shown in Fig. 1.

As illustrated in Fig. 1, the Young's modulus E is assumed to vary exponentially along the longitudinal and thickness directions, in the form of

$$E(x, z) = E_0 e^{\alpha z + \beta x} \quad (1)$$

where E_0 is assumed to be a constant, while α and β are the inhomogeneity parameters along z and x axes, respectively. Meanwhile, the Poisson's ratio ν remains constant, independent of any coordinate variable.

With the plane stress assumption, the two-dimensional constitutive relations are

$$\begin{Bmatrix} \sigma_x \\ \sigma_z \\ \tau_{xz} \end{Bmatrix} = \frac{E(x, z)}{1 - \nu^2} \begin{bmatrix} 1 & \nu & 0 \\ \nu & 1 & 0 \\ 0 & 0 & (1 - \nu)/2 \end{bmatrix} \begin{Bmatrix} \partial u_x / \partial x \\ \partial u_z / \partial z \\ \partial u_x / \partial z + \partial u_z / \partial x \end{Bmatrix} \quad (2)$$

where σ_x , σ_z , and τ_{xz} are the normal and shear stresses, and u_x and u_z are the displacements in the x - and z -direction. For plane-strain problem, we should replace $E(x, z)$ by $E(x, z)/(1 - \nu^2)$ and ν by $\nu/(1 - \nu)$.

In the absence of body forces, the equations of equilibrium are

$$\frac{\partial \sigma_x}{\partial x} + \frac{\partial \tau_{xz}}{\partial z} = 0, \quad \frac{\partial \tau_{xz}}{\partial x} + \frac{\partial \sigma_z}{\partial z} = 0 \quad (3)$$

To facilitate the analysis in subsequent subsections, the following new stress variables are introduced

$$\hat{\sigma}_x = \sigma_x e^{-\alpha z - \beta x}, \quad \hat{\sigma}_z = \sigma_z e^{-\alpha z - \beta x}, \quad \hat{\tau}_{xz} = \tau_{xz} e^{-\alpha z - \beta x} \quad (4)$$

Making use of Eqs. (2) and (3), we can derive the matrix state equation as

$$\frac{\partial \mathbf{v}}{\partial z} = \mathbf{H} \mathbf{v} \quad (5)$$

where $\mathbf{v} = [u_z, u_x, \hat{\sigma}_z, \hat{\tau}_{xz}]^T$ is the state vector and the operator matrix \mathbf{H} is given by

$$\mathbf{H} = \begin{bmatrix} 0 & -\nu \frac{\partial}{\partial x} & \frac{1-\nu^2}{E_0} & 0 \\ -\frac{\partial}{\partial x} & 0 & 0 & \frac{2(1+\nu)}{E_0} \\ 0 & 0 & -\alpha & -\beta - \frac{\partial}{\partial x} \\ 0 & -E_0 \frac{\partial^2}{\partial x^2} - E_0 \beta \frac{\partial}{\partial x} & -\nu \frac{\partial}{\partial x} - \nu \beta & -\alpha \end{bmatrix} \quad (6)$$

When the inhomogeneous parameters equal zero, the operator matrix \mathbf{H} becomes the same as the conventional Hamiltonian operator matrix for homogenous materials (Yao *et al.* 2009).

3. Symplectic framework

In this section, a brief review of the symplectic approach for bi-directional functionally graded materials problems with lateral traction-free boundary conditions is given firstly. Then, a particular solution for plane beams subjected to arbitrary form tractions on the upper and lower surfaces is presented. The two ends of the beam are subjected to the combinations of the boundary conditions as below:

- (1) Simply supported end: $\sigma_z=0, u_x=0$
- (2) Clamped end: $u_z=0, u_x=0$
- (3) Free end: $\sigma_z=0, \tau_{xz}=0$

As the plane problem has been reformulated in the state space, the method of separation of variables along with the eigenfunction expansion technique is employed to reduce the original problems to analyzing eigenvalues and their eigensolutions. The complete elasticity solution for generally supported beam is formed by eigensolutions of the homogeneous problem and particular solution corresponding to nonhomogeneous boundary conditions on the lateral surfaces.

To obtain the general solutions for the bi-directional FGM beam, we consider the following homogenous boundary conditions on the lateral surfaces as

$$x = \pm h: \hat{\sigma}_x = E_0 \frac{\partial u_x}{\partial x} + \nu \hat{\sigma}_z = 0, \quad \hat{\tau}_{xz} = 0 \quad (7)$$

The method of separation of variables is possible for Eq. (5)

$$\mathbf{v}(x, z) = \xi(z) \mathbf{\Phi}(x) = \xi(z) [w(x), u(x), \sigma(x), \tau(x)]^T \quad (8)$$

Substitution of Eq. (8) into Eq. (5), we can get

$$\frac{\dot{\xi}(z)}{\xi(z)} = \frac{[\mathbf{H}\mathbf{\Phi}(x)]_i}{[\mathbf{\Phi}(x)]_i} = \mu \quad (9)$$

where $\mathbf{\Phi}(x) = (\Phi_1(x) \ \Phi_2(x) \ \dots \ \Phi_n(x))^T$. Eq. (9) leads to an analytical solution about the variation with z

$$\xi(z) = e^{\mu z} \quad (10)$$

and gives rise to the eigen-equation

$$\mathbf{H}\mathbf{\Phi}(x) = \mu \mathbf{\Phi}(x) \quad (11)$$

where μ is the eigenvalue of the operator matrix \mathbf{H} , and $\mathbf{\Phi}(x)$ is the corresponding eigenvector.

Similar to the analytical procedure of axial functionally graded materials (Zhao *et al.* 2012b), we can derive that zero and $-\alpha$ are the eigenvalues of the operator matrix \mathbf{H} . It can also be found that, if μ is an eigenvalue of \mathbf{H} , then $-\mu-\alpha$ is also an eigenvalue. It should be noted that the stresses for two particular eigenvalues 0 and $-\alpha$ do not decay exponentially with z and the solutions are known as the Saint-Venant solutions, while the stresses for other eigenvalues ($\mu \neq 0, -\alpha$) vary exponentially with z and the solutions are usually dominant only near the ends of a beam.

The eigenvalues of the operator matrix \mathbf{H} can be divided into two classes:

(1) **Particular eigenvalues:** zero and $-\alpha$, which are multiple, their fundamental eigensolutions and Jordan form eigensolutions need to be considered respectively.

(2) **General eigenvalues:** μ_i and $-\mu_i-\alpha$ are the conjugate pair of eigenvalues. All eigenvalues can be divided into two groups of (a) and (b) as follows

$$(a)\text{-group: } \mu_{-i}, \quad \text{Re}(\mu_i) < -\alpha/2 \quad \text{or} \quad \text{Re}(\mu_i) = -\alpha/2 \quad \cap \quad \text{Im} \mu_i < 0 \quad (i = 1, 2, \dots, n). \quad (12a)$$

$$(b)\text{-group: } \mu_{-i} = -\mu_i - \alpha \quad (12b)$$

3.1 The eigensolutions of eigenvalues zero and $-\alpha$

From the eigen-Eq. (11), explicit expressions of the eigenvectors and eigensolutions for eigenvalues zero and $-\alpha$ are obtainable.

When $\mu=0$, the eigen-equation becomes $\mathbf{H}\mathbf{\Phi}(x)=0$ and the corresponding eigenvectors are

$$\mathbf{\Phi}_{0,1}^{(0)} = [1, 0, 0, 0]^T, \quad \mathbf{\Phi}_{0,2}^{(0)} = [0, 1, 0, 0]^T, \quad \mathbf{\Phi}_{0,2}^{(1)} = [-x, 0, 0, 0]^T \quad (13)$$

Similarly, the eigenvectors of the eigenvalue $-\alpha$ can be obtained as

$$\mathbf{\Phi}_{-\alpha,1}^{(0)} = \left[-\cosh(\lambda x) / \alpha, -\lambda \sinh(\lambda x) / (\alpha^2), E_0 \cosh(\lambda x), 0 \right]^T$$

$$\mathbf{\Phi}_{-\alpha,2}^{(0)} = \left[\sinh(\lambda x) / (\lambda \alpha), \cosh(\lambda x) / \alpha^2, -E_0 \sinh(\lambda x) / \lambda, 0 \right]^T$$

$$\Phi_{-\alpha}^{(1)} = \left(\begin{array}{l} \left\{ \xi_1 \frac{x \cosh(\lambda x)}{\lambda^2} - \xi_2 \beta \frac{x \sinh(\lambda x)}{\lambda} + \xi_4 \frac{\sinh(\lambda x)}{\lambda^3} + 2\xi_2 \beta \frac{C_0}{E_0} e^{-\beta x} \right. \\ \left. + A_0 \xi_2 \left[(\beta x + 1) \cosh(\lambda x) - \xi_3 \frac{x \sinh(\lambda x)}{\lambda} + \frac{\beta}{\lambda} \sinh(\lambda x) \right] \right\} \\ \frac{1}{\alpha} \left\{ \xi_1 \left[\frac{x \sinh(\lambda x)}{\lambda} - \frac{2 \cosh(\lambda x)}{\lambda^2} \right] - \xi_2 \beta \left[x \cosh(\lambda x) - \frac{\sinh(\lambda x)}{\lambda} \right] - 2\xi_2 \lambda^2 \frac{C_0}{E_0} e^{-\beta x} \right. \\ \left. + A_0 \left[\xi_2 \beta \lambda x \sinh(\lambda x) - \xi_1 x \cosh(\lambda x) \right] \right\} \\ E_0 \alpha \left\{ \frac{\xi_1}{\lambda^2} \left[\frac{\sinh(\lambda x)}{\lambda} - x \cosh(\lambda x) \right] + \xi_2 \beta \frac{x \sinh(\lambda x)}{\lambda} - 2 \frac{C_0}{E_0} \beta \xi_2 e^{-\beta x} \right. \\ \left. + A_0 \frac{\xi_1}{\lambda^2} \left[\lambda x \sinh(\lambda x) + \cosh(\lambda x) \right] - A_0 \xi_2 \beta \left[x \cosh(\lambda x) + \frac{\sinh(\lambda x)}{\lambda} \right] \right\} \\ E_0 \left\{ \frac{\lambda \cosh(\lambda x) - \beta \sinh(\lambda x)}{\lambda(\lambda^2 - \beta^2)} + \frac{C_0}{E_0} e^{-\beta x} - A_0 \frac{\lambda \sinh(\lambda x) - \beta \cosh(\lambda x)}{(\lambda^2 - \beta^2)} \right\} \end{array} \right) \quad (14)$$

in which $\lambda = \alpha\sqrt{\nu}$. It should be noted that the first subscripts 0 and $-\alpha$ in Eq.(14) indicate the eigenvalues zero and $-\alpha$, the second subscripts 1 and 2 indicate the first and second Jordan chain, the superscripts (0) and (1) indicate the fundamental eigenvectors and first order Jordan normal form eigenvectors, respectively. Meanwhile, it should be noted that $\Phi_{-\alpha}^{(1)}$ has been determined by means of Jordan chain $H\Phi_{-\alpha}^{(1)} = -\alpha\Phi_{-\alpha}^{(1)} + \Phi_{-\alpha}^{(0)}$, in which $\Phi_{-\alpha}^{(0)}$ was reconstructed as (Zhao *et al.* 2012c)

$$\Phi_{-\alpha}^{(0)} = A_0 \Phi_{-\alpha,1}^{(0)} + \Phi_{-\alpha,2}^{(0)} \quad (15)$$

where $C_0 = E_0 \sinh(\lambda h) \cosh(\lambda h) / \{ \lambda [\beta \cosh(\lambda h) \sinh(\beta h) - \lambda \sinh(\lambda h) \cosh(\beta h)] \}$ and $A_0 = [\beta \sinh(\lambda h) \cosh(\beta h) - \lambda \cosh(\lambda h) \sinh(\beta h)] / \{ \lambda [\beta \cosh(\lambda h) \sinh(\beta h) - \lambda \sinh(\lambda h) \cosh(\beta h)] \}$. The coefficients ξ_i ($i=1,2,3,4$) are listed in Appendix A.

The eigensolutions corresponding to the zero eigenvalue can be constructed as

$$\mathbf{v}_{0,1}^{(0)} = \Phi_{0,1}^{(0)}, \quad \mathbf{v}_{0,2}^{(0)} = \Phi_{0,2}^{(0)}, \quad \mathbf{v}_{0,2}^{(1)} = \Phi_{0,2}^{(1)} + z\Phi_{0,2}^{(0)} = [-x, z, 0, 0]^T \quad (16)$$

The original solutions of the original homogeneous problem corresponding to eigenvalue $-\alpha$ are

$$\mathbf{v}_{-\alpha,1}^{(0)} = \mathbf{M}_t e^{-\alpha z} \Phi_{-\alpha,1}^{(0)}, \quad \mathbf{v}_{-\alpha,2}^{(0)} = \mathbf{M}_t e^{-\alpha z} \Phi_{-\alpha,2}^{(0)}, \quad \mathbf{v}_{-\alpha}^{(1)} = \mathbf{M}_t e^{-\alpha z} (\Phi_{-\alpha}^{(1)} + z\Phi_{-\alpha}^{(0)}) \quad (17)$$

where $\mathbf{M}_t = \text{diag}[1, 1, e^{\alpha z + \beta x}, e^{\alpha z + \beta x}]$ is the transform (diagonal) matrix between the eigensolution and the original solution.

3.2 General eigensolutions

To obtain the eigensolutions of the general eigenvalues ($\mu \neq 0, -\alpha$), we can assume the solution of the eigen-equation $H\Phi(x) = \mu\Phi(x)$ in the form of

$$\Phi(x) = e^{\eta x} \mathbf{V} \quad (18)$$

where V is an undetermined constant vector, and η is the eigen-root of the following characteristic polynomial

The eigen-root η can be obtained as

$$\begin{aligned} \eta_1 &= -\frac{1}{2}\beta + \frac{1}{2}\alpha\sqrt{v} + \frac{1}{2}\sqrt{\beta^2 + v\alpha^2 - 2\alpha\beta\sqrt{v} - 4\mu(\mu + \alpha + \beta\sqrt{v})} \\ \eta_2 &= -\frac{1}{2}\beta + \frac{1}{2}\alpha\sqrt{v} - \frac{1}{2}\sqrt{\beta^2 + v\alpha^2 - 2\alpha\beta\sqrt{v} - 4\mu(\mu + \alpha + \beta\sqrt{v})} \\ \eta_3 &= -\frac{1}{2}\beta - \frac{1}{2}\alpha\sqrt{v} + \frac{1}{2}\sqrt{\beta^2 + v\alpha^2 + 2\alpha\beta\sqrt{v} - 4\mu(\mu + \alpha - \beta\sqrt{v})} \\ \eta_4 &= -\frac{1}{2}\beta - \frac{1}{2}\alpha\sqrt{v} - \frac{1}{2}\sqrt{\beta^2 + v\alpha^2 + 2\alpha\beta\sqrt{v} - 4\mu(\mu + \alpha - \beta\sqrt{v})} \end{aligned} \tag{19}$$

The corresponding eigen-vector can be written as

$$w = \sum_{i=1}^4 A_i e^{\eta_i x}, \quad u = \sum_{i=1}^4 B_i e^{\eta_i x}, \quad \sigma = \sum_{i=1}^4 C_i e^{\eta_i x}, \quad \tau = \sum_{i=1}^4 D_i e^{\eta_i x} \tag{20}$$

Substituting the eigen-vector in Eq. (20) into eigen-equation $H\Phi(x) = \mu\Phi(x)$, the relations between coefficients A_i, B_i, C_i and D_i are

$$\begin{cases} C_i = -\frac{\eta_i + \beta}{\alpha + \mu} D_i \\ B_i = \frac{1}{E_0 \mu^2} \left[\frac{\eta_i (\eta_i + \beta)}{\alpha + \mu} + (2\mu + \mu v - \alpha v) + \frac{\beta v}{\eta_i + \beta} (\alpha + \mu) \right] D_i, \quad (i = 1, 2, 3, 4) \\ A_i = \frac{1}{E_0 \mu (\eta_i + \beta)} \left[v(\alpha + \mu) - \frac{(\eta_i + \beta)^2}{\alpha + \mu} \right] D_i \end{cases} \tag{21}$$

Thus, a nontrivial solution D_i ($i=1,2,3,4$) can be deduced from homogeneous boundary conditions on the lateral surfaces as follows

$$\left. \begin{aligned} D_{1n} &= E_0 \mu_n (\alpha + \mu_n) \\ D_{2n} &= \frac{(\eta_{2n} + \beta)(\eta_{3n} - \eta_{1n})}{(\eta_{1n} + \beta)(\eta_{2n} - \eta_{3n})} \frac{e^{(\eta_{1n} - \eta_{4n})h} - e^{(\eta_{4n} - \eta_{1n})h}}{e^{(\eta_{2n} - \eta_{4n})h} - e^{(\eta_{4n} - \eta_{2n})h}} D_{1n} \\ D_{3n} &= \frac{(\eta_{3n} + \beta)(\eta_{2n} - \eta_{1n})}{(\eta_{1n} + \beta)(\eta_{3n} - \eta_{2n})} \frac{e^{(\eta_{1n} - \eta_{4n})h} - e^{(\eta_{4n} - \eta_{1n})h}}{e^{(\eta_{3n} - \eta_{4n})h} - e^{(\eta_{4n} - \eta_{3n})h}} D_{1n} \\ D_{4n} &= \frac{(\eta_{4n} + \beta)(\eta_{2n} - \eta_{1n})}{(\eta_{1n} + \beta)(\eta_{2n} - \eta_{4n})} \frac{e^{(\eta_{1n} - \eta_{3n})h} - e^{(\eta_{3n} - \eta_{1n})h}}{e^{(\eta_{3n} - \eta_{4n})h} - e^{(\eta_{4n} - \eta_{3n})h}} D_{1n} \end{aligned} \right\} \tag{22}$$

Then, the general eigenvalue μ can be obtained from the following transcendental equation

$$\begin{aligned} &(\eta_1 - \eta_2)(\eta_3 - \eta_4) \cosh(2\lambda h) + (\eta_1 - \eta_4)(\eta_2 - \eta_3) \cosh[(\eta_1 - \eta_2 - \eta_3 + \eta_4)h] \\ &+ (\eta_1 - \eta_3)(\eta_4 - \eta_2) \cosh[(\eta_1 - \eta_2 + \eta_3 - \eta_4)h] = 0 \end{aligned} \tag{23}$$

Thus, the eigen-solution and the corresponding original solution for any particular eigenvalue μ_n can be obtained as

$$\mathbf{v}_n = e^{\mu_n z} \boldsymbol{\Phi}_n, \quad \mathbf{v}'_n = \mathbf{M}_l \mathbf{v}_n \quad (24)$$

in which the components of $\boldsymbol{\Phi}_n$ are given in Eq. (20).

3.3 Particular solutions

Next, we investigate the particular solutions for bi-directional FGM beams subjected to arbitrary form tractions on the lateral surfaces. The conditions at the upper and lower surfaces are assumed as

$$\begin{aligned} x = -h : (\tilde{\sigma}_x =) E_0 \frac{\partial \tilde{u}}{\partial x} + v \tilde{\sigma} &= q_1(z) e^{-\alpha z + \beta h}, \quad \tilde{\tau} = 0 \\ x = h : (\sigma_x =) E_0 \frac{\partial \tilde{u}}{\partial x} + v \tilde{\sigma} &= q_2(z) e^{-\alpha z - \beta h}, \quad \tilde{\tau} = 0 \end{aligned} \quad (25)$$

Following similarly the procedure presented in literature (Zhao and Gan 2015), the displacement and stress components of the particular solution $\tilde{\boldsymbol{\Phi}}$ are obtained from the equation $\mathbf{H}\tilde{\boldsymbol{\Phi}} = -\alpha\tilde{\boldsymbol{\Phi}} + k\boldsymbol{\Phi}_{-\alpha}^{(1)}$ as

$$\begin{aligned} \tilde{w} &= \frac{k}{\alpha v} \left\{ \frac{m_5}{4} \left[x^2 \sinh(\lambda x) + \frac{x \cosh(\lambda x)}{\lambda} - \frac{\sinh(\lambda x)}{2\lambda^2} \right] + \frac{m_6}{4} \left[x^2 \cosh(\lambda x) + \frac{x \sinh(\lambda x)}{\lambda} - \frac{\cosh(\lambda x)}{2\lambda^2} \right] \right. \\ &+ \frac{m_7}{2} \left[x \cosh(\lambda x) + \frac{\sinh(\lambda x)}{2\lambda} \right] + \frac{m_8}{2} \left[x \sinh(\lambda x) + \frac{\cosh(\lambda x)}{2\lambda} \right] + \left(\frac{\xi_1}{\lambda^2} + A_0 \xi_2 \beta \right) v x \cosh(\lambda x) \\ &- (\beta + A_0 \xi_1) \xi_2 v \frac{x \sinh(\lambda x)}{\lambda} + (A_0 \xi_2 v - \xi_6) \cosh(\lambda x) + \left[\left(A_0 \xi_2 \beta + \frac{\xi_4}{\lambda^2} \right) \frac{v}{\lambda} + \xi_5 \right] \sinh(\lambda x) \\ &+ \left(m_9 \beta x - m_9 \frac{\lambda^2 + \beta^2}{\beta^2 - \lambda^2} + m_{10} \beta \right) \frac{e^{\beta x}}{\beta^2 - \lambda^2} + \left[(1 - v^2)(C_0 x - D) + 2C_0 \xi_2 \beta v \right] \frac{e^{-\beta x}}{E_0} \left. \right\} \\ \tilde{u} &= \frac{k}{4\lambda} \left\{ m_5 x^2 \cosh(\lambda x) + m_6 x^2 \sinh(\lambda x) + \left(2m_7 - \frac{m_5}{\lambda} \right) x \sinh(\lambda x) + \left(2m_8 - \frac{m_6}{\lambda} \right) x \cosh(\lambda x) \right. \\ &+ \left(\frac{m_5}{2\lambda} - m_7 \right) \frac{\cosh(\lambda x)}{\lambda} + \left(\frac{m_6}{2\lambda} - m_8 \right) \frac{\sinh(\lambda x)}{\lambda} + 4\lambda \left[m_9 \left(x - \frac{2\beta}{\beta^2 - \lambda^2} \right) + m_{10} \right] \frac{e^{\beta x}}{\beta^2 - \lambda^2} \left. \right\} \\ \tilde{\sigma} &= \frac{kE_0}{v} \left\{ \frac{m_5}{4\lambda} \left[\frac{\sinh(\lambda x)}{2\lambda} - x \cosh(\lambda x) - \lambda x^2 \sinh(\lambda x) \right] + \frac{m_6}{4\lambda} \left[\frac{\cosh(\lambda x)}{2\lambda} - x \sinh(\lambda x) - \lambda x^2 \cosh(\lambda x) \right] \right. \\ &- \frac{m_7}{2} \left[x \cosh(\lambda x) + \frac{\sinh(\lambda x)}{2\lambda} \right] - \frac{m_8}{2} \left[x \sinh(\lambda x) + \frac{\cosh(\lambda x)}{2\lambda} \right] + \frac{(\beta + A_0 \lambda^2)}{(\lambda^2 - \beta^2)^2} \left[\cosh(\lambda x) - \frac{\beta}{\lambda} \sinh(\lambda x) \right] \\ &- \frac{(1 + A_0 \beta)}{(\lambda^2 - \beta^2)^2} \left[\lambda \sinh(\lambda x) - \beta \cosh(\lambda x) \right] + \left(m_9 \beta x + m_9 \frac{\lambda^2 + \beta^2}{\lambda^2 - \beta^2} + m_{10} \beta \right) \frac{e^{\beta x}}{\lambda^2 - \beta^2} + (D - C_0 x) \frac{e^{-\beta x}}{E_0} \left. \right\} \\ \tau &= kE_0 \left\{ \alpha \left[-m_1 x \cosh(\lambda x) + m_2 x \sinh(\lambda x) - m_3 \cosh(\lambda x) + m_4 \sinh(\lambda x) \right] + (2\xi_2 C_0 \alpha \beta x + F) \frac{e^{-\beta x}}{E_0} \right\} \end{aligned} \quad (26)$$

in which $D = [q_1(z) + q_2(z)]e^{-\alpha z} / (2k) + E_0 [\xi_7 \sinh(\lambda h) \sinh(\beta h) / \lambda - \xi_8 \cosh(\lambda h) \cosh(\beta h)] / (\lambda^2 - \beta^2)^2$
 $k = [q_1(z) - q_2(z)]e^{-\alpha z} / \{2E_0 [\xi_7 \sinh(\lambda h) \cosh(\beta h) / \lambda - \xi_8 \cosh(\lambda h) \sinh(\beta h)] / (\lambda^2 - \beta^2)^2 + 2C_0 h\}$, and
 $F = E_0 \alpha [-m_2 h \sinh(\lambda h) + m_3 \cosh(\lambda h) + 2C_0 \xi_2 \beta h \sinh(\beta h) / E_0] / \cosh(\beta h)$.

The coefficients ξ_i and m_i in Eq. (26) are listed in Appendix A.

The particular solution of the original plane problem can be constructed as

$$\tilde{v} = M_i e^{-\alpha z} \left\{ \tilde{\Phi} + k \left[z \Phi_{-\alpha}^{(1)} + \frac{1}{2} z^2 (A_0 \Phi_{-\alpha,1}^{(0)} + \Phi_{-\alpha,2}^{(0)}) \right] \right\} \quad (27)$$

The elasticity solutions of bi-directional functionally graded beams with various boundary conditions are formed by eigensolutions of eigenvalues zero and $-\alpha$, general eigensolutions and the particular solution mentioned above. The complete analytical solution can be described as

$$v = \tilde{v} + c_1 v_{0,1}^{(0)} + c_2 v_{0,2}^{(0)} + c_3 v_{0,2}^{(1)} + c_4 v_{-\alpha,1}^{(0)} + c_5 v_{-\alpha,2}^{(0)} + c_6 v_{-\alpha}^{(1)} + \sum_{i=1}^N (a_i v_i' + b_i v_{-i}') \quad (28)$$

It should be mention that N is a truncated number, which should be large enough to make sure the accuracy of the symplectic expansion. The unknown constants c_i ($i=1,2,\dots,6$), a_i and b_i can be determined by a linear system of equations resulted from the Hamiltonian variational principle as follows (Leung and Zheng 2007)

$$E \{m\} = F - G \quad (29)$$

where $m = [c_1, c_2, c_3, c_4, c_5, c_6, a_k, b_k \ (k=1,2,\dots,N)]^T$ and

$$E_{ij} = \int_{-h}^h \{ [\sigma_i(u_x)_j + \tau_i(u_z)_j]_{x=0} - [\sigma_j(u_x)_i + \tau_j(u_z)_i]_{x=0} - [\sigma_i(u_x)_j + \tau_i(u_z)_j]_{x=l} + [\sigma_j(u_x)_i + \tau_j(u_z)_i]_{x=l} \} dz$$

$$F_i = \int_{-h}^h \{ [\sigma_i(\bar{u}_x)_0 + \tau_i(\bar{u}_z)_0]_{x=0} - [\bar{\sigma}_0(u_x)_i + \bar{\tau}_0(u_z)_i]_{x=0} - [\sigma_i(\bar{u}_x)_l + \tau_i(\bar{u}_z)_l]_{x=l} + [\bar{\sigma}_l(u_x)_i + \bar{\tau}_l(u_z)_i]_{x=l} \} dz$$

$$G_i = \int_{-h}^h \{ [\sigma_i \tilde{u}_x + \tau_i \tilde{u}_z]_{x=0} - [\tilde{\sigma}(u_x)_i + \tilde{\tau}(u_z)_i]_{x=0} - [\sigma_i \tilde{u}_x + \tau_i \tilde{u}_z]_{x=l} + [\tilde{\sigma}(u_x)_i + \tilde{\tau}(u_z)_i]_{x=l} \} dz$$

$(i=1,2,\dots,N+6; j=1,2,\dots,N+6)$

Take the simple supported beam as example, the boundary conditions at $z=0$ and $z=l$ are

$$\begin{aligned} x=0: \bar{u}_x &= 0, \bar{\sigma}_z = 0 \\ x=l: \bar{u}_x &= 0, \bar{\sigma}_z = 0 \end{aligned} \quad (30)$$

In order to accord with Eq. (29), the boundary conditions above can be expressed as

$$\begin{aligned} x=0: (\bar{u}_x)_0 &= 0, \bar{\sigma}_0 = 0 \\ x=l: (\bar{u}_x)_l &= 0, \bar{\sigma}_l = 0 \end{aligned} \quad (31)$$

Substituting Eq. (31) into the Eq. (29), the coefficients c_i , a_k and b_k can be determined.

4. Numerical examples

4.1 Example 1

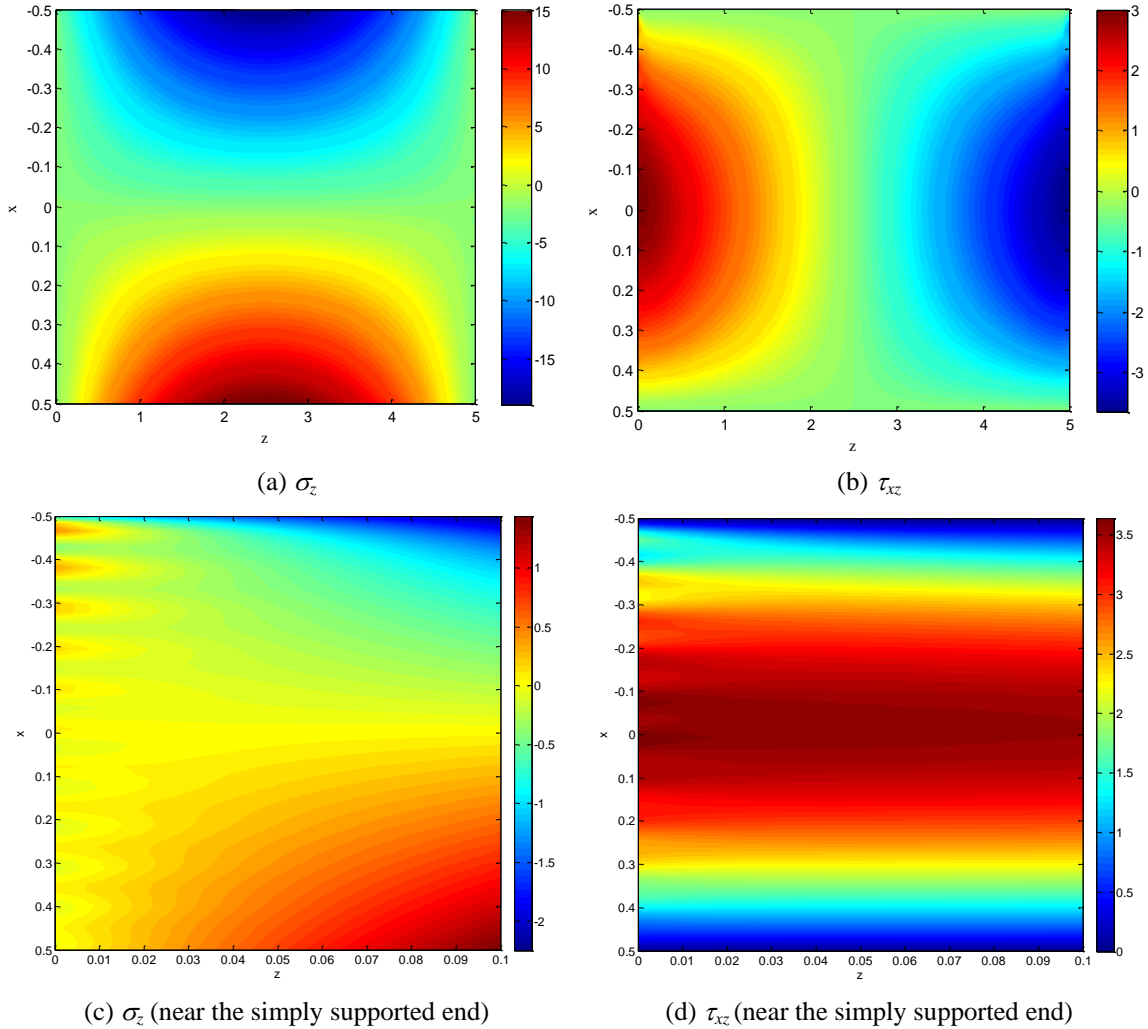


Fig. 2 Contours of normal and shear stresses for homogenous beam ($ah=0$, $\beta h=0$)

Consider the plane stress problem of the simple supported isotropic beam of thickness $2h=1$ m and length-to-thickness ratio $l/(2h)=5$, which is subjected to prescribed normal tractions $q_1=-10$ (kN/m) at its upper surface. The Young's modulus varies exponentially both along the z - and x -axes with its value at the point $O(0,0)$ being $E_0=2.0\times 10^{11}$ N/m², and the Poisson's ratio $\nu=0.29$ keeps constant. The axial material gradient index ah and the transverse one βh are investigated in details. The unit of normal and shear stresses in the contour plots is 1.0×10^4 N/m, the same as that of the normal and shear stresses distributing along the length direction.

In Figs. 2-5, Figs. (a) and (b) show the contours of normal and shear stresses for whole beams, while Figs. (c) and (d) display the local normal and shear stresses near the simply supported end. Besides, Fig. 6 below presents the distributions of normal and shear stresses along longitudinal direction. It should be noted that the numerical example emphasizes on the effectiveness of symplectic approach in obtaining analytical elasticity solutions. Only particular solution, six

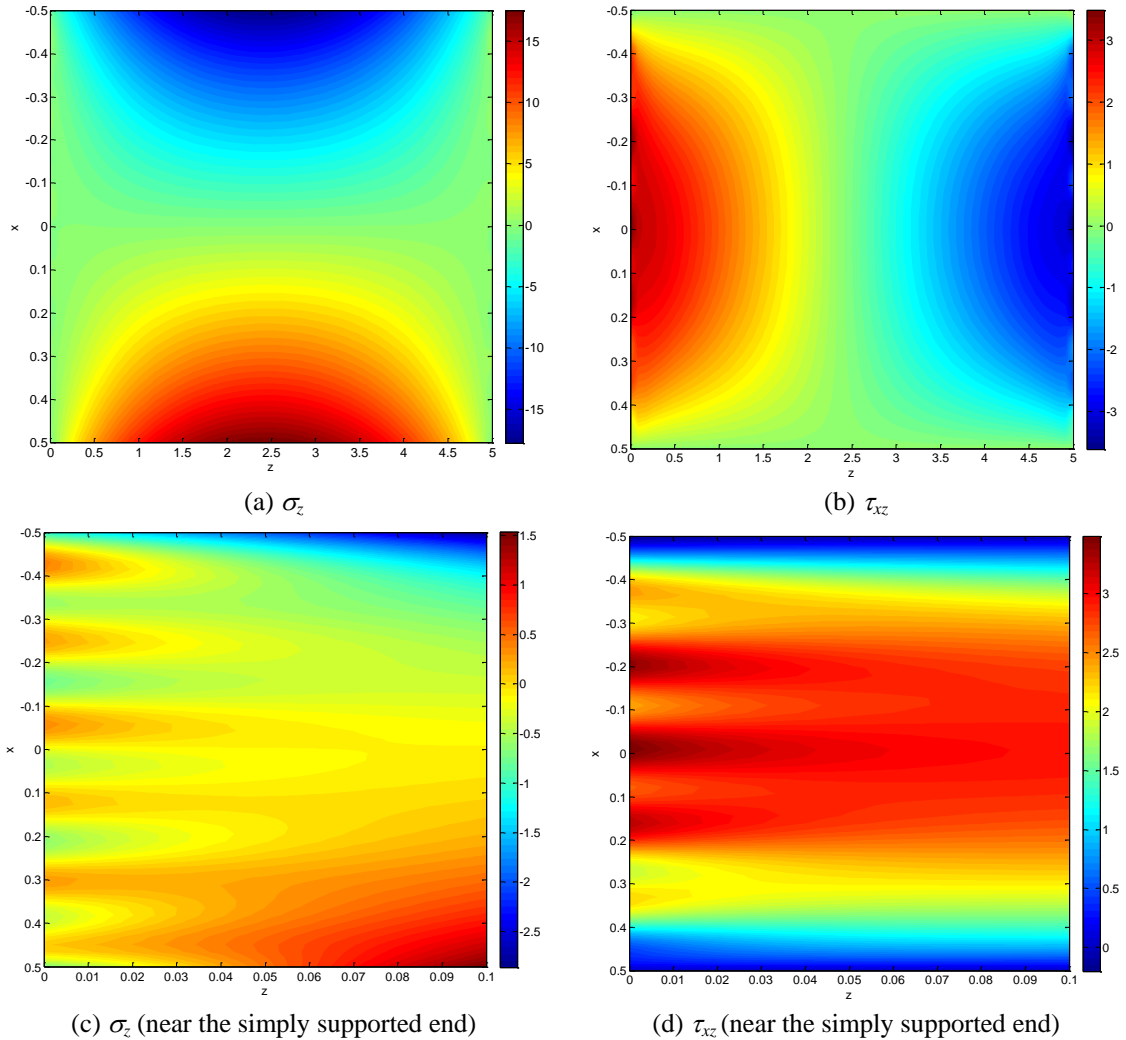


Fig. 3 Contours of normal and shear stresses for axial FGM beam ($ah=0.01, \beta h=0$)

particular eigensolutions and 40 general eigensolutions in Eq. (28) are retained to ensure the computational efficiency in the numerical examples.

Fig. 2 (a) and (b) display the contours of normal and shear stresses for homogeneous beam ($ah=0, \beta h=0$), which agree well with the solutions in Timoshenko and Goodier (1970). To obtain highly accurate local stress and displacement distributions, e.g., at the simply supported end, general eigen-solutions have also be taken into consideration. Fig. 2 (c) and (d) show the local contours of normal and shear stresses near the simply supported end ($0 \leq z \leq 0.1$). It can be seen from Fig. 2(c) that, the normal stress on the simply supported end fluctuates around zero, but does not vanish. The symplectic approach involves the expansion in terms of eigensolutions and the truncated number N does influence on the accuracy of the symplectic expansion. Another reason may be the numerical error due to the limited precision of the floating-point representation of a numerical quantity imposed by the digital computer.

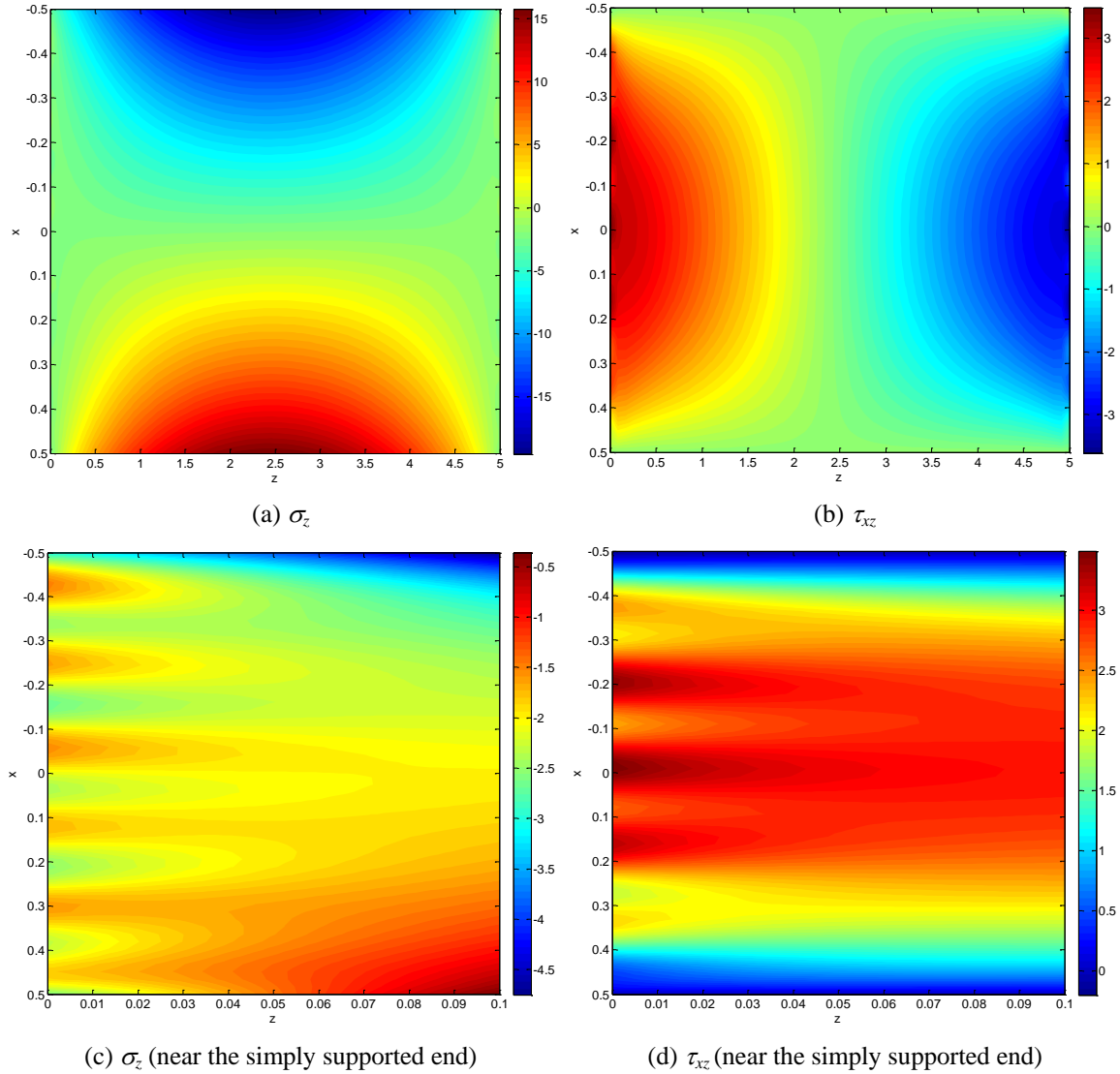


Fig. 4 Contours of normal and shear stresses for bi-directional FGM beam ($ah=0.01$, $\beta h=1 \times 10^{-10}$)

When the transverse gradient index β equals zero, the bi-directional FGM beam degenerates to the conventional axial FGM beam ($ah=0.01$, $\beta h=0$). The normal and shear stresses distributions of the functionally graded beam are displayed in Fig. 3 (a) and (b), which match excellently with the corresponding results in Zhao and Gan (2015).

For comparison, the stress contours are also presented in Fig. 4 for bi-directional functionally graded beam with transverse gradient index β approaching zero ($ah=0.01$, $\beta h=1 \times 10^{-10}$). It can be seen from Figs. 2-4 that, the well matches of stress distributions are obtained for the smaller inhomogeneous parameters $ah=0.01$ and $\beta h=1 \times 10^{-10}$. Hereto, the capability of the symplectic framework developed in bi-directional FGM beam has been assessed.

The contours of normal and shear stresses for bi-directional FGM beam with material gradient

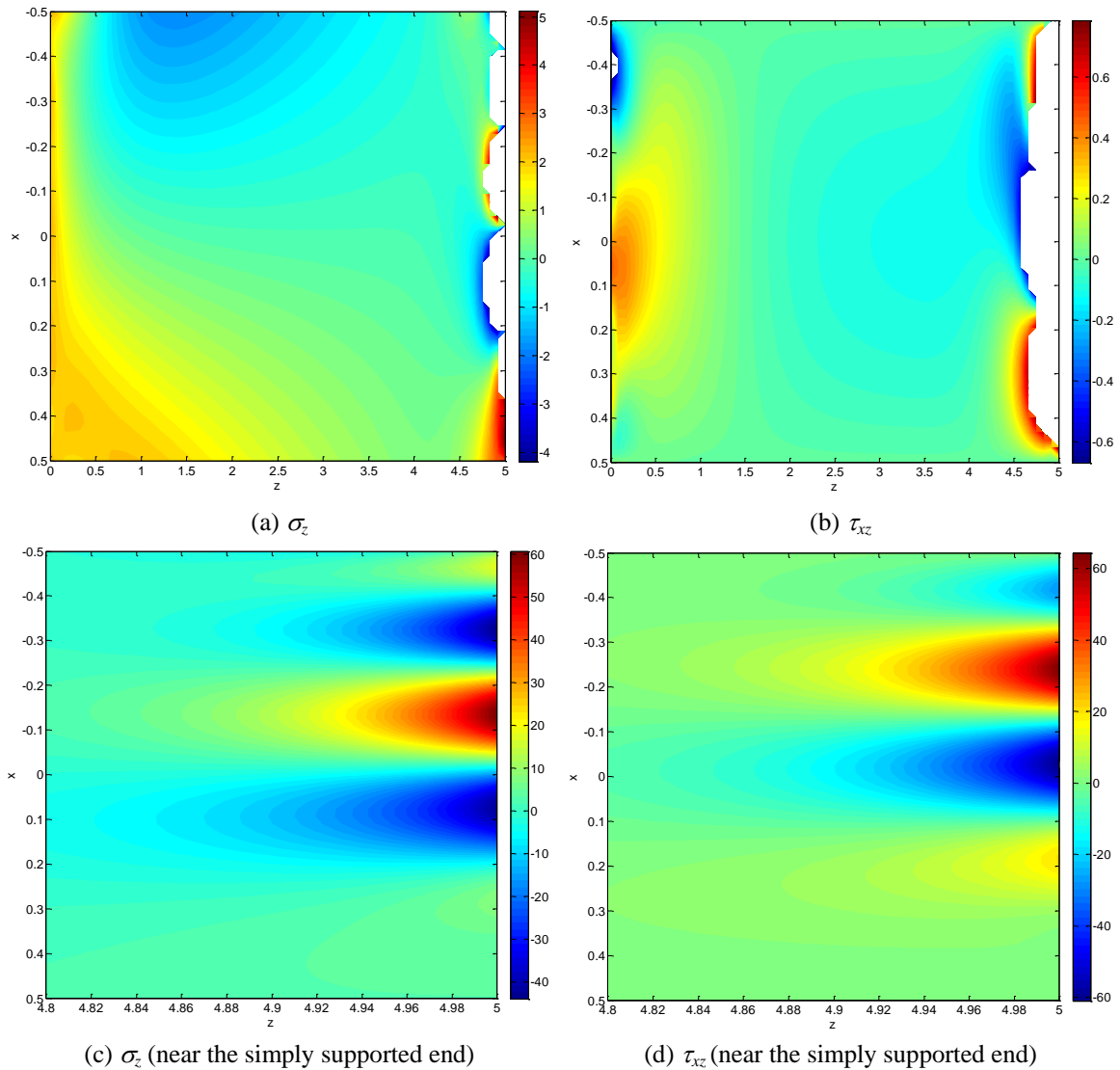
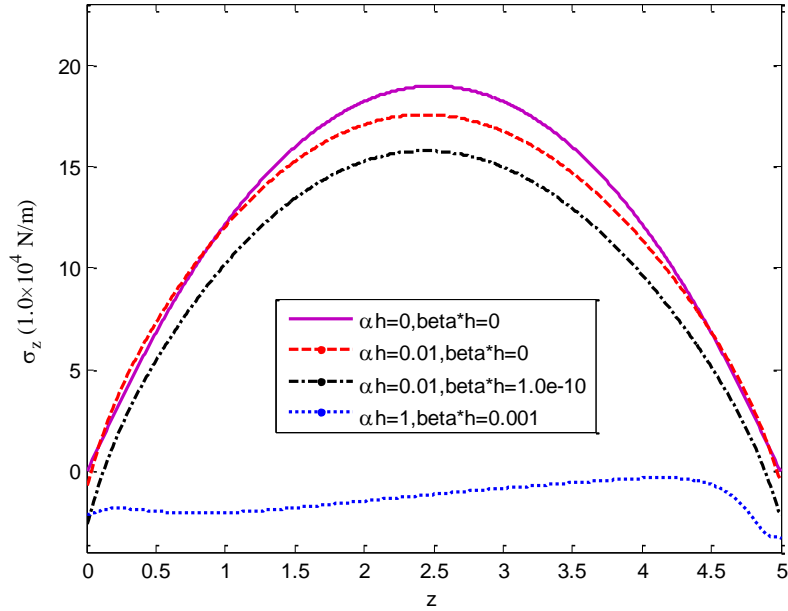


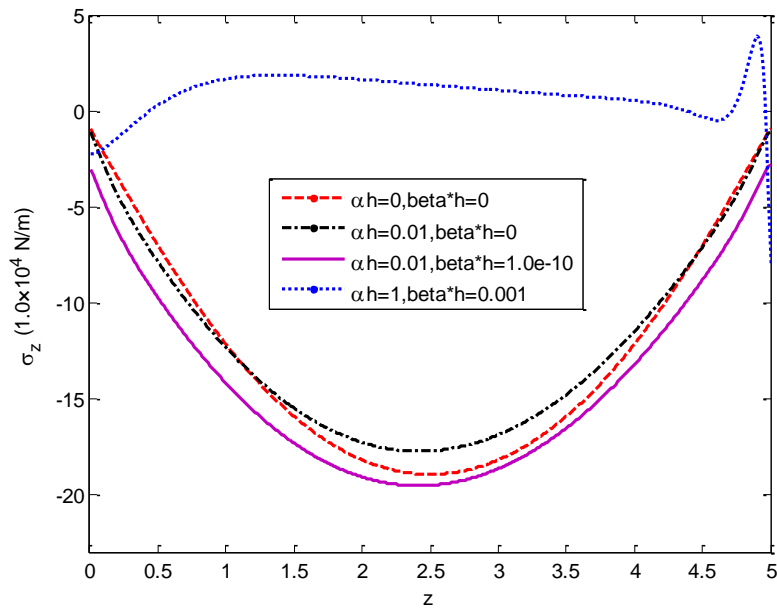
Fig. 5 Contours of normal and shear stresses for bi-directional FGM beam ($ah=1, \beta h=0.001$)

indices $ah=1$ and $\beta h=0.001$ are given in Fig. 5 which are obvious different from the ones in Figs. 2-4. From the figures, we can find that the material inhomogeneities do have a significant influence on the elastic field in the strip.

For comparison, Fig. 6 (a) and (b) present the distributions of normal stress at $x=0.5$ and at $x=-0.5$ along the longitudinal direction, respectively. While Fig. 6(c) display the shear stress distribution at $x=0$ along the longitudinal direction. It is obvious that, when the material inhomogeneity parameters ah and βh both take extremely small value, the normal and shear stresses are similar to that of the homogenous materials ($ah=0, \beta h=0$). When the axial inhomogeneity parameter $ah=1$, the normal and shear results begin to deviate obviously from those of the homogenous material.



(a) The normal stress distribution at $x=0.5$

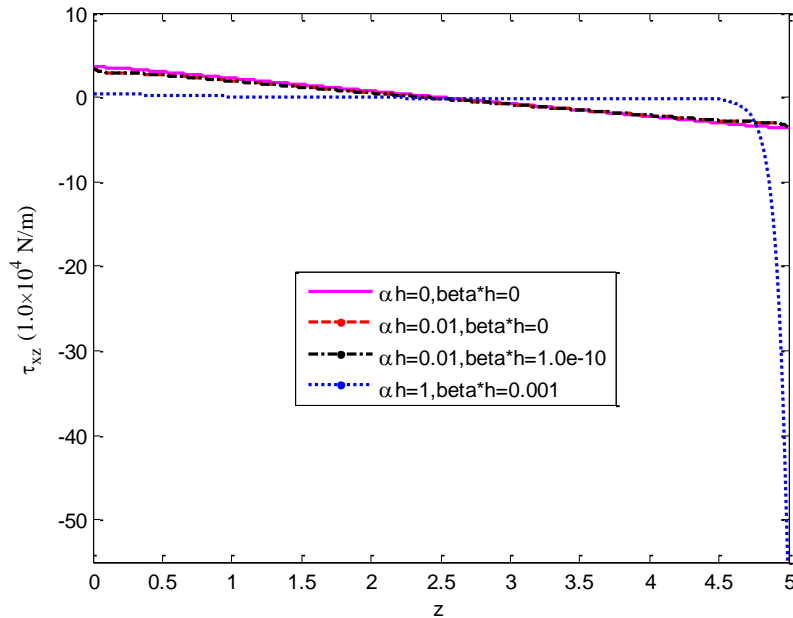


(b) The normal stress distribution at $x=-0.5$

Fig. 6 The normal and shear stress distribution along the longitudinal direction

4.2 Example 2

Consider the cantilever bi-directional FGM beam with the length $l=5$ m and the thickness $2h=1$ m, subjected to a linear normal traction $q(z)=-q_0(z-2l)/l$ ($q_0=1000$ kN/m) at its upper surface



(c) The shear stress distribution at $x=0$

Fig. 6 Continued

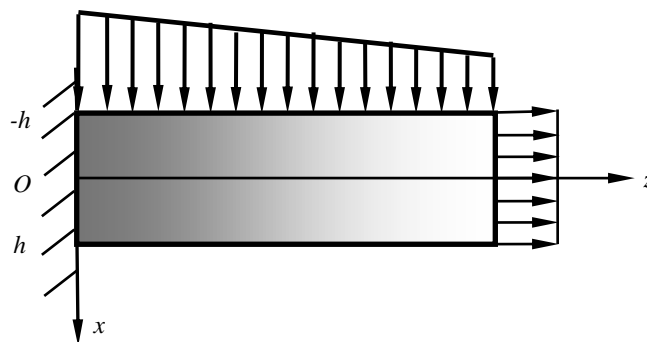


Fig. 7 The bi-directional FGM cantilever beam subjected to distribution lateral loads

and a prescribed simple tensile stress $\tilde{\sigma}_t = 100(\text{kN/m})$ at the free end. The Poisson's ratio ν and parameter E_0 are the same with those of the bi-directional FGM beam in example 1. The transverse material gradient index is taken to be $\beta h = 0.00001$, and the axial one takes the values $ah = -0.2$ and $ah = -0.1$.

The contours of stress and displacement for homogeneous material are showed in Fig. 8 which accord with the solutions of classical elasticity theory (Timoshenko and Goodier 1970). Fig. 9 displays the contours of stress and displacement for clamped-free bi-directional FGM beam ($ah = -0.2$, $\beta h = 0.00001$) by expansion of Eq. (28). The results are obtained by retaining particular solution and 36 eigen-solutions in the expansion. It can be seen from Fig. 9 that, the symplectic

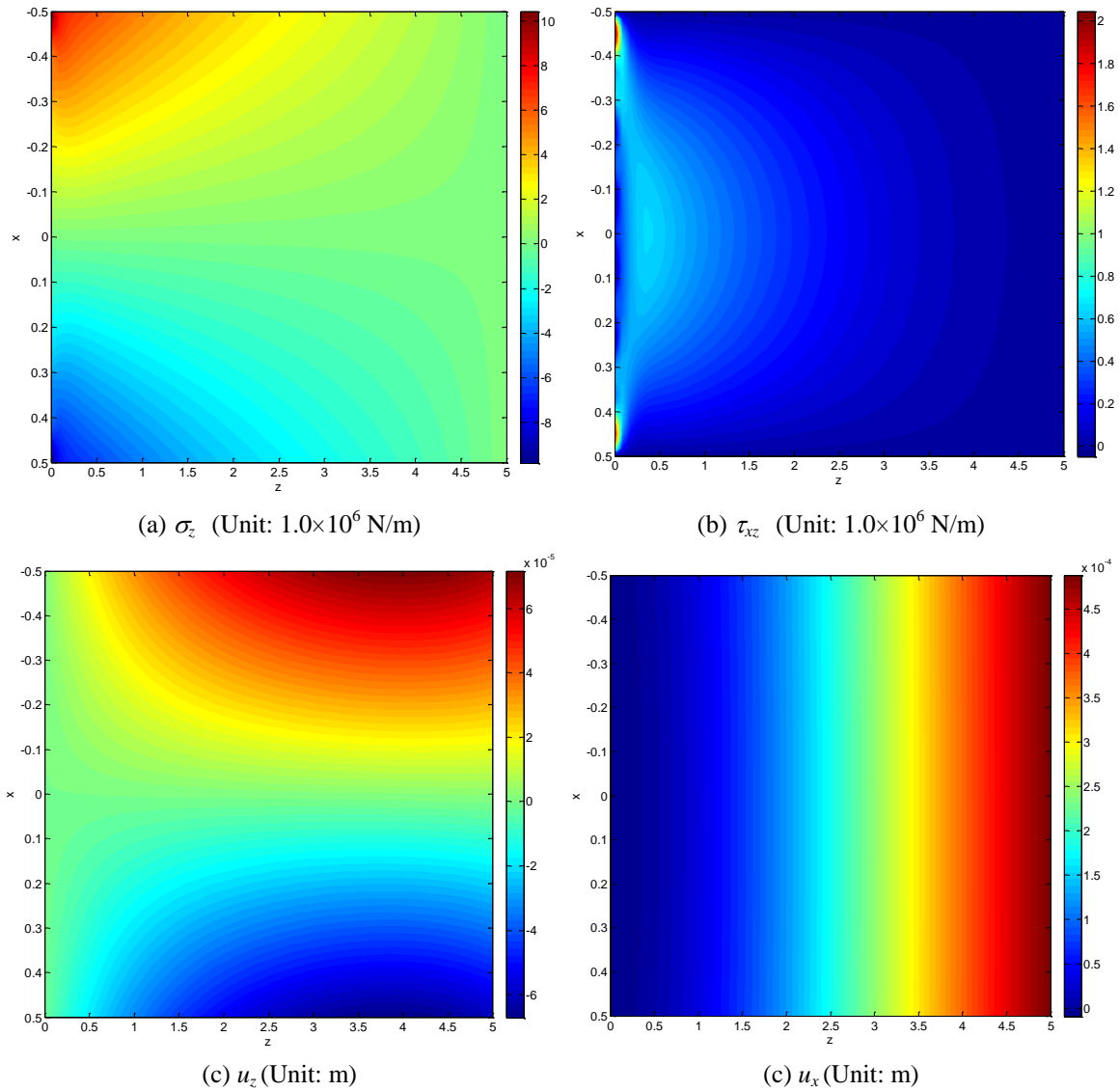


Fig. 8 Contours of stress and displacement for homogeneous material beam ($\alpha h=0, \beta h=0$)

framework enable us to obtain the highly accurate local stress and displacement distributions, especially at the clamped end of the cantilever beam.

For comparison, Fig. 10 suggests that the bi-directional FGM beam with a small material gradient index ($\alpha h=-0.1, \beta h=0.00001$) behaves more reasonable for normal and shear stresses at the vicinity of clamped end. It is seen from Figs. 9 and 10 that, the axial gradient index αh plays an obvious effect on the normal and shear stress distributions. The influence of the transverse gradient index can also be investigated similarly when necessary. These essential results indicate that the selection of material gradient indices of the bi-directional FGM beams can be tailored to meet the desired goals in practice engineering.

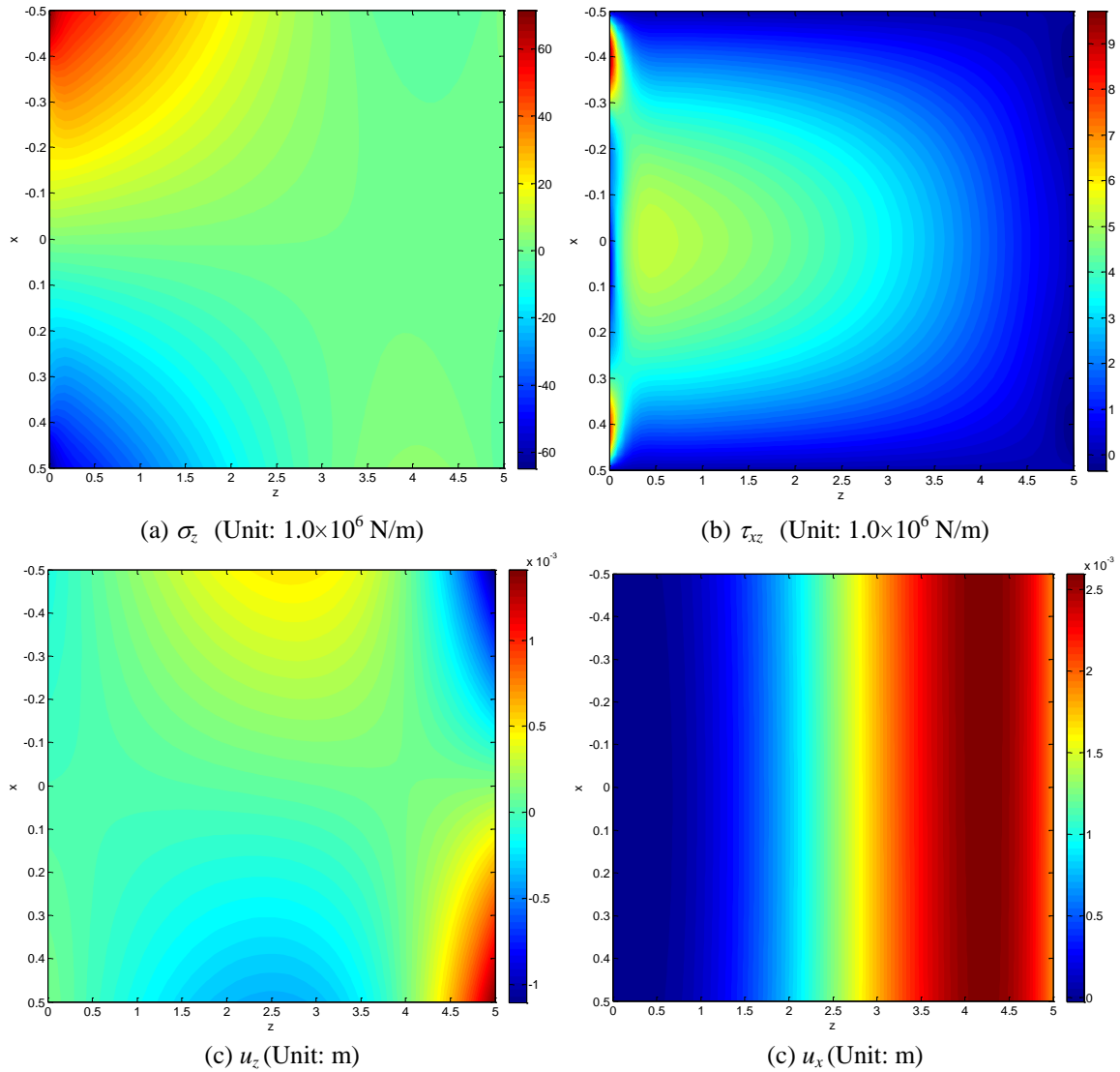


Fig. 9 Contours of stress and displacement for bi-directional FGM beam ($ah=-0.2, \beta h=0.00001$)

Table 1 Normal stress σ_z at $x=-0.5$ along the longitudinal direction

Material gradient index	Length coordinate (m)										
	0	0.5	1.0	1.5	2.0	2.5	3.0	3.5	4.0	4.5	5.0
$ah=0$ $\beta h=0$	10.4359	6.1776	5.1149	4.2119	3.4710	2.8500	2.3041	1.7882	1.2573	0.6677	-0.0384
$ah=-0.1$ $\beta h=0.0001$	32.5920	21.9455	18.5557	15.2624	12.3697	9.9517	8.0417	6.6577	5.7911	5.3834	7.2901
$ah=-0.2$ $\beta h=0.00001$	71.6405	48.2017	37.9374	28.0233	18.9330	10.9716	4.4793	-0.1591	-2.5266	-2.1604	2.7039

Note: The unit of normal stress σ_z is 1.0×10^6 N/m.

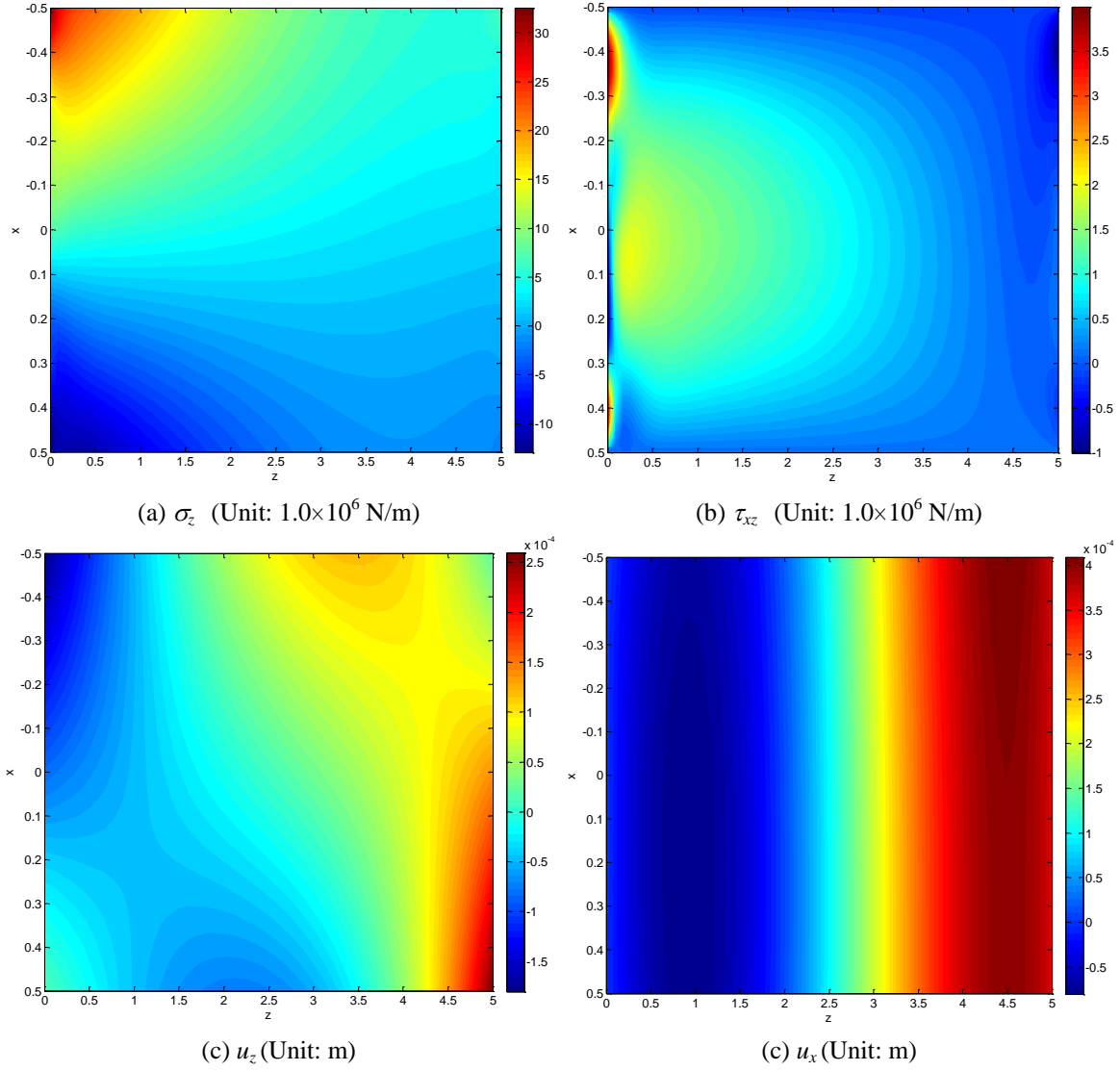


Fig. 10 Contours of stress and displacement for bi-directional FGM beam ($ah=-0.1, \beta h=0.00001$)

Table 2 Normal stress σ_z at $x=0.5$ along the longitudinal direction

Material gradient index	Length coordinate (m)										
	0	0.5	1.0	1.5	2.0	2.5	3.0	3.5	4.0	4.5	5.0
$ah=0$ $\beta h=0$	-9.8275	-6.0472	-4.9449	-4.0340	-3.2902	-2.6664	-2.1176	-1.5988	-1.0650	-0.4724	0.2355
$ah=-0.1$ $\beta h=0.0001$	-12.2641	-11.2153	-8.4630	-6.0918	-4.1721	-2.6958	-1.6727	-1.0966	-0.9439	-1.1673	-1.8646
$ah=-0.2$ $\beta h=0.00001$	-64.7702	-43.2337	-33.1484	-23.5908	-14.9387	-7.4743	-1.5393	2.4805	4.1747	3.1206	-2.5332

Different from Fig. 6, Tables 1 and 2 present the values of normal stress at eleven points along the longitudinal direction at $x=-0.5$ and at $x=0.5$, respectively. The results in bold correspond to the homogenous materials and are calculated within symplectic framework (Zhao and Gan 2015). From the comparison, we can see that the axial gradient index αh plays a significant influence on the normal stress distribution in the strip.

5. Conclusions

The symplectic approach based on Hamiltonian system was effectively extended to obtain exact elasticity solutions for bi-directional FGM beams subjected to arbitrary distributed lateral loads. Considering homogenous boundary conditions on the lateral surface, the eigensolutions of two special eigenvalues (zero and $-\alpha$) and general eigenvalues ($\mu \neq 0$, $-\alpha$) were obtained from eigen-function. Furthermore, a particular solution satisfying the lateral distribution loads on the upper and bottom surface was derived in a systematic manner. The complete analytical solution is obtained by the theorem of superposition. Numerical results reveal that the present approach is effective and accurate in predicting local stress distributions. From the numerical investigation, it can also be concluded that the material gradient indices play a significant influence on the stresses of the bi-directional FGM beams. Furthermore, maximum value and uniformity of stress distributions can be modified to a required manner by selecting appropriate material properties.

It should be noted that, the present symplectic scheme can be established a well-structured analytical procedure for functionally graded beams with material properties varying respectively exponentially in the length or thickness direction, and also for bi-directional functionally graded beams with material properties varying exponentially in both length and thickness directions. But for functionally graded beams with material properties varying arbitrarily, numerical technique is necessary to facilitate numerical solution in the symplectic framework. Besides, further endeavors could be made to seek numerical solutions for bi-directional FGM beams subjected to concentrated force and other type of discontinuous loads on the lateral surfaces.

Acknowledgments

This work is supported by the National Natural Science Foundation of China (Nos. 11202111, 11572287 and 51378266), Natural Science Foundation of Zhejiang Province (No. LY15A020006), the Natural Science Foundation of Ningbo City (No. 2015A610295) and Zhejiang Open Foundation of the Most Important Subjects.

References

- Chu, P., Li, X.F., Wu, J.X. and Lee, K.Y. (2015), "Two-dimensional elasticity solution of elastic strips and beams made of functionally graded materials under tension and bending", *Acta Mech.*, **226**(7), 2235-2253.
- Ding, H.J., Huang, D.J. and Chen, W.Q. (2007), "Elasticity solutions for plane anisotropic functionally graded beams", *Int. J. Solid. Struct.*, **44**(1), 176-196
- Ebrahimi, M.J. and Najafizadeh, M.M. (2014), "Free vibration analysis of two-dimensional functionally graded cylindrical shells", *Appl. Math. Model.*, **38**, 308-324.
- Ferreira, A.J.M., Batra, R.C., Roque, C.M.C., Qian, L.K. and Jorge, R.M.N. (2006), "Natural frequencies of

- functionally graded plates by a meshless method”, *Compos. Struct.*, **75**, 593-600.
- Hedia, H.S. (2005), “Comparison of one-dimensional and two-dimensional functionally graded materials for the backing shell of the cemented acetabular cup”, *J. Biomed. Mater. Res.: Part B. Appl. Biomater.*, **74B**(2), 732-739.
- Huang, D.J., Ding, H.J. and Chen, W.Q. (2009), “Analytical solution and semi-analytical solution for anisotropic functionally graded beam subject to arbitrary loading”, *Sci. China Ser. G: Phys. Mech Astron.*, **52**(8), 1244-1256.
- Huang, Y. and Li, X.F. (2011), “Buckling analysis of nonuniform and axially graded columns with varying flexural rigidity”, *J. Eng. Mech.*, **137**(1), 73-81.
- Khalili, S.M.R., Jafari, A.A. and Eftekhari, S.A. (2010), “A mixed Ritz-DQ method for forced vibration of functionally graded beams carrying moving loads”, *Compos. Struct.*, **92**, 2497-2511.
- Koizumi, M. (1993), “The concept of FGM”, *Trans. Am. Ceram. Soc.*, **34**, 3-10.
- Koizumi, M. (1997), “FGM activities in Japan”, *Compos. Part B: Eng.*, **28**(1-2), 1-4.
- Kuo, H.Y. and Chen, T.Y. (2005), “Steady and transient Green’s functions for anisotropic conduction in an exponentially graded solid”, *Int. J. Solid. Struct.*, **42**(3-4), 1111-1128.
- Leung, A.Y.T. and Zheng, J.J. (2007), “Closed form stress distribution in 2D elasticity for all boundary conditions”, *Appl. Math. Mech. Eng. Ed.*, **28**(12), 1629-1642.
- Lezgy-Nazargah, M. (2015), “Fully coupled thermo-mechanical analysis of bi-directional FGM beams using NURBS isogeometric finite element approach”, *Aero. Sci. Tech.*, **45**, 154-164.
- Lü, C.F., Chen, W.Q., Xu, R.Q. and Lim, C.W. (2008), “Semi-analytical elasticity solutions for bi-directional functionally graded beams”, *Int. J. Solid. Struct.*, **45**(1), 258-275.
- Lü, C.F., Lim, C.W. and Chen, W.Q. (2009), “Semi-analytical analysis for multi-directional functionally graded plates: 3-D elasticity solutions”, *Int. J. Numer. Meth. Eng.*, **79**(1), 25-44.
- Nemat-Alla, M. (2003), “Reduction of thermal stresses by developing two-dimensional functionally graded materials”, *Int. J. Solid. Struct.*, **40**(26), 7339-7356.
- Neves, A.M.A., Ferreira, A.J.M., Carrera, E., Roque, C.M.C., Cinefra, M. and Jorge R.M.N. (2011), “Bending of FGM plates by a sinusoidal plate formulation and collocation with radial basis functions”, *Mech. Res. Commun.*, **38**(5), 368-371.
- Nie, G. and Zhong, Z. (2010), “Dynamic analysis of multi-directional functionally graded annular plates”, *Appl. Math. Model.*, **34**, 608-616.
- Qian, L.F. and Batra, R.C. (2005), “Design of bidirectional functionally graded plate for optimal natural frequencies”, *J. Sound Vib.*, **280**(1-2), 415-424.
- Reddy, J.N. (2000), “Analysis of functionally graded plates”, *Int. J. Numer. Meth. Eng.*, **47**, 663-684.
- Sallai, B.O., Tounsi, A., Mechab, I., Bachir, B.M., Meradjah, M. and Adda Bedia, E.A. (2009), “A theoretical analysis of flexional bending of Al/Al₂O₃ S-FGM thick beams”, *Comput. Mater. Sci.*, **44**, 1344-1350.
- Sankar, B.V. (2001), “An elastic solution for functionally graded beams”, *Compos. Sci. Technol.*, **61**(5), 689-696.
- Shahba, A. and Rajasekaran, S. (2012), “Free vibration and stability of tapered Euler-Bernoulli beams made of axially functionally graded materials”, *Appl. Math. Model.*, **36**(7), 3094-3111.
- Shahba, A., Attarnejad, R. and Hajilar, S. (2012), “A mechanical-based solution for axially functionally graded tapered Euler-Bernoulli beams”, *Mech. Adv. Mater. Struct.*, **20**(8), 696-707.
- Shahba, A., Attarnejad, R. and Hajilar, S. (2011), “Free vibration and stability of axially functionally graded tapered Euler-Bernoulli beams”, *Shock & Vibration*, **18**(5), 683-696.
- Shahba, A., Attarnejad, R., Marvi, M.T. and Hajilar, S. (2011), “Free vibration and stability analysis of axially functionally graded tapered Timoshenko beams with classical and non-classical boundary conditions”, *Compos. Part B: Eng.*, **42**, 801-808.
- Shariyat, M. and Alipour, M.M. (2013), “A power series solution for vibration and complex modal stress analyses of variable thickness viscoelastic two-directional FGM circular plates on elastic foundations”, *Appl. Math. Model.*, **37**, 3063-3076.
- Simsek, M. and Cansiz, S. (2012), “Dynamics of elastically connected double-functionally graded beam

- systems with different boundary conditions under action of a moving harmonic load”, *Compos. Struct.*, **94**, 2861-2878.
- Simsek, M. (2009), “Static analysis of a functionally graded beam under a uniformly distributed load by Ritz method”, *Int. J. Eng. Appl. Sci.*, **1**, 1-11.
- Simsek, M. (2015), “Bi-directional functionally graded materials (BDFGMs) for free and forced vibration of Timoshenko beams with various boundary conditions”, *Compos. Struct.*, **133**, 968-978.
- Simsek, M. and Reddy, J.N. (2013), “A unified higher order beam theory for buckling of a functionally graded microbeam embedded in elastic medium using modified couple stress theory”, *Compos. Struct.*, **101**, 47-58.
- Simsek, M., Kocatürk, T. and Akbas, S.D. (2013), “Static bending of a functionally graded microscale Timoshenko beam based on the modified couple stress theory”, *Compos. Struct.*, **95**, 740-747.
- Sobhani Aragh, B., Hedayati, H., Borzabadi Farahani, E. and Hedayati, M. (2011), “A novel 2-D six-parameter power-law distribution for free vibration and vibrational displacements of two-dimensional functionally graded fiber-reinforced curved panels”, *Eur. J. Mech. A/Solid.*, **30**, 865-883.
- Sutradhar, A. and Paulino, G.H. (2004), “The simple boundary element method for transient heat conduction in functionally graded material”, *Comp. Meth. Appl. Mech. Eng.*, **193**(42-44), 4511-4539.
- Timoshenko, S.P. and Goodier, J.N. (1970), *Theory of Elasticity*, McGraw-Hill, New York, NY, USA.
- Yao, W.A., Zhong, W.X. and Lim, C.W. (2009), *Symplectic Elasticity*, World Scientific Publishing Company, New Jersey, USA.
- Zhao, L. and Wei, Z.G. (2015), “Analytical solutions for functionally graded beams under arbitrary distribution loads via the symplectic approach”, *Advan. Mech. Eng.*, Article ID, 321263.
- Zhao, L., Chen, W.Q. and Lü, C.F. (2012a), “New assessment on the Saint-Venant solutions for functionally graded materials beams”, *Mech. Res. Commun.*, **43**, 1-6.
- Zhao, L., Chen, W.Q. and Lü, C.F. (2012b), “Two-dimensional complete rational analysis of functionally graded beams within symplectic framework”, *Appl. Math. Mech. Eng. Ed.*, **33**(10), 1225-1238.
- Zhao, L., Chen, W.Q. and Lü, C.F. (2012c), “Symplectic elasticity for bi-directional functionally graded materials”, *Mech. Mater.*, **54**, 32-42.
- Zhong, W.X. (1995), *A New Systematic Methodology for Theory of Elasticity*, Dalian University of Technology Press, Dalian, DL, China. (in Chinese)

Appendix A

$$\begin{aligned}
\xi_1 &= (\beta^2\nu + \lambda^2) / (\lambda^2 - \beta^2), \quad \xi_2 = (1 + \nu) / (\lambda^2 - \beta^2), \\
\xi_3 &= (\beta^2\nu + \lambda^2) / (1 + \nu), \quad \xi_4 = [\lambda^2(\nu - 1) - 2\beta^2\nu] / (\lambda^2 - \beta^2), \\
\xi_5 &= (1 - \nu^2) [(\beta / \lambda + A_0\lambda)\beta + (1 + A_0\beta)\lambda] / (\lambda^2 - \beta^2)^2, \\
\xi_6 &= (1 - \nu^2) [(\beta / \lambda + A_0\lambda)\lambda + (1 + A_0\beta)\beta] / (\lambda^2 - \beta^2)^2, \\
\xi_7 &= (\lambda^2 + \beta^2) + 2\beta A_0\lambda^2, \quad \xi_8 = 2\beta + A_0(\lambda^2 + \beta^2), \\
m_1 &= [\beta(\xi_1 / \lambda^2 + \xi_2) + A_0(\xi_1 + \xi_2\beta^2)] / (\lambda^2 - \beta^2), \\
m_2 &= [A_0\lambda\beta(\xi_1 / \lambda^2 + \xi_2) + (\xi_1 + \xi_2\beta^2) / \lambda] / (\lambda^2 - \beta^2), \\
m_3 &= [(\xi_1 + \xi_2\beta^2)(2 + A_0\beta) + A_0(\xi_1 / \lambda^2 + \xi_2)\beta^3] / (\lambda^2 - \beta^2)^2, \\
m_4 &= \beta [(1 + A_0\beta)[2\xi_1 + \xi_2(\beta^2 + \lambda^2)] + \xi_1(\lambda^2 - \beta^2) / \lambda^2] / [\lambda(\lambda^2 - \beta^2)^2], \\
m_5 &= 2[(1 + \nu)\lambda^2 m_2 - \xi_1\nu / \lambda - A_0\xi_2\beta\lambda\nu], \quad m_6 = [2\xi_2\nu\beta + A_0\xi_2\nu(\xi_1 + \xi_3) - 2(1 + \nu)\lambda^2 m_1], \\
m_7 &= (\xi_1 - \xi_4) / \alpha^2 - A_0\xi_2\nu\beta - 2(1 + \nu)\lambda^2 m_3 - \xi_5\lambda, \quad m_8 = A_0\xi_2\nu(\xi_1 / \lambda - \lambda) + 2(1 + \nu)\lambda^2 m_4 + \xi_6\lambda, \\
m_9 &= C_0\beta(1 + \nu) [4\xi_2\lambda^2 + (1 - \nu)] / E_0, \quad m_{10} = [2\xi_2\nu(\beta^2 + \lambda^2)C_0 - (1 - \nu^2)(C_0 + \beta D) + 2\alpha\nu(1 + \nu)F] / E_0
\end{aligned}$$